arXiv:quant-ph/0605010v2 3 May 2006

Quantum teleportation over the Swisscom telecommunication network

Olivier Landry *, J.A.W. van Houwelingen, Alexios Beveratos, Hugo Zbinden, and Nicolas Gisin
Group of Applied Physics, University of Geneva,
20 rue de l'École-de-médecine, 1205 Genève, Switzerland

We present a quantum teleportation experiment in the quantum relay configuration using the installed telecommunication network of Swisscom. In this experiment, the Bell state measurement occurs well after the entanglement has been distributed, at a point where the photon upon which data is teleported is already far away, and the entangled qubits are photons created from a different crystal and laser pulse than the teleported qubit. A raw fidelity of 0.93±0.04 has been achieved using a heralded single-photon source.

INTRODUCTION

Quantum teleportation, or the ability to transfer information in the form of qubits between two locations without a direct quantum channel, has many practical applications in addition to its fundamental significance. In quantum communication protocols, such as quantum key distribution [1, 2], the maximum distance one can reach is limited by channel losses and detector noise. When the signal to noise ratio gets lower than a certain limit which depends on the choice of protocol and experimental details, no secure information can be retrieved. While the losses in optical fibers cannot be decreased with current technologies, a suitably designed communication channel making use of quantum relays[3, 4] or quantum repeaters[5] can reduce the noise and therefore increase the distance limit. Quantum relays uses quantum teleportation and entanglement swapping to perform a kind of quantum non-demolition measurement at some points within the channel, in effect measuring the presence of a photon without measuring the qubit it carries. Detectors can then be opened only when a photon is certain to arrive, reducing dark counts, the main source of noise. Quantum repeaters perform the same task but also use quantum memories and entanglement purification.

In previous experiments, teleportation was demonstrated inside a laboratory[6, 7, 8] or in the field but without prior entanglement distribution[9]. The Bell-State Measurement always took place before the third photon was distributed to Bob. On the other hand, in all these experiments the same laser pulse was used to create both the entangled pair and the photon to be teleported. These two points limit the feasibility of a practical quantum relay and open conceptual loopholes. Here we present an experiment where teleportation occurs long after entanglement distribution and the photons involved originate from two crystals excited by different pulses from the same laser.

*email: olivier.landry@physics.unige.ch

PROTOCOL

The quantum teleportation protocol [10] (schematically described in fig 1) requires that Bob (the receiver) and Charlie (a third party) share an entangled state, which in this case is a $|\phi^+\rangle$ state. Alice (the sender) needs to send a qubit over to Bob, but does not possess a direct quantum channel. She sends it to Charlie who performs a Bell State measurement[11] using a beamsplitter and classically announces the result to Bob.

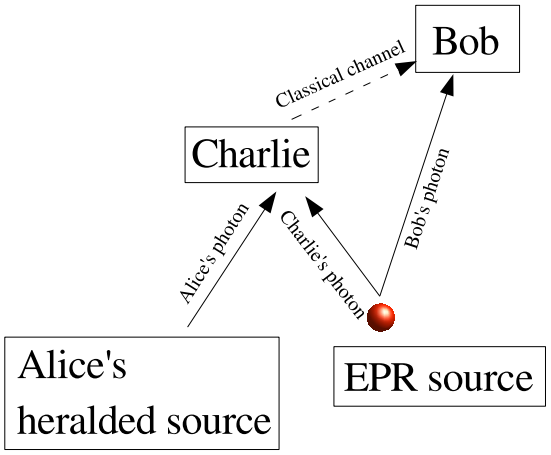


FIG. 1: The teleportation protocol. Quantum channels are in plain lines, classical channels are in dashed lines. The state that Bob measures is the same that Alice sent to Charlie up to a unitary transformation. EPR source is a source of entangled states, or Einstein-Podolsky-Rosen states [12].

Time-bin qubits

Time-bin qubits [13] have proven to be very robust against decoherence in optical fibers[14] and several long distance experiments have been demonstrated[8, 15, 16]. In this experiment time-bin qubits lying on the equator of the Bloch sphere are created using an unbalanced interferometer. For a review of time-bin qubits see Tittel and Weihs[17].

SETUP

The experimental setup is shown in fig. 2. A mode-locked Ti:Sapphire laser (Mira Coherent, pumped using a Verdi laser) creates 185 fs pulses with a spectral width of 4 nm at a central wavelength of 711 nm, a mean power of 400mW and a repetition rate of 75 MHz. This beam is split in two parts using a variable coupler ($\lambda/2$ and a polarization beamsplitter).

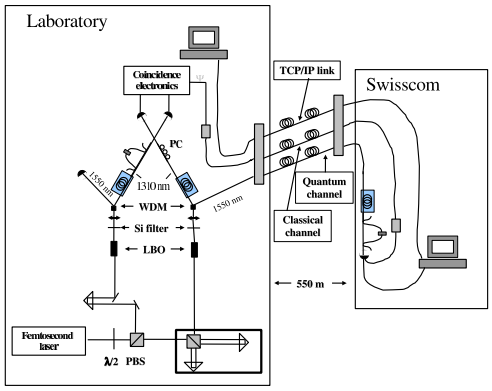


FIG. 2: The optical circuit. PC: Polarization controller. QM: rudimentary Quantum Memory (fiber spools).

The transmitted light is sent through an unbalanced Michelson interferometer stabilized using a frequency-stabilized HeNe laser (Spectra Physics 117A) and then on a Lithium Borite (LBO) non-linear crystal (NLC) cut for type-I phase-matching, which creates a time-bin entangled photon pair in the $|\phi^+\rangle$ state by spontaneous parametric downconversion. The created photons have wavelengths of 1310 and 1555 nm and are easily separated using a wavelength division multiplexer (WDM). A Si filter is used to remove the remaining 711 nm light.

Charlie's photon

The 1310 nm photon is sent in a 179.72 m spool of fiber. This spool serves as a rudimentary quantum memory (QM). While Charlie's part of the entangled qubit pair is waiting in this spool, Bob's part leaves the laboratory.

Alice's photon

Alice prepares her photon using the light reflected from the variable coupler. A pair of photons is created in the same type of crystal as above, then separated. The 1555 nm photon can either be discarded or detected by an InGaAs APD in order to herald the photon to be teleported[18, 19]. If it is not detected, teleportation still occurs without other changes in the setup.

The 1310 nm photon is stored in a 177 m spool of fiber. The 2.72 m difference with Charlie's QM corresponds exactly to the spacing between two subsequent pulses of the laser. This means that Alice's photon upon which the qubit to be teleported will be encoded is produced from a different pulse of the laser than Charlie's and Bob's photons. This is a conceptually important step towards completely independant laser sources[20, 21].

In order to encode a qubit on her photon, Alice sends it after the spool to an unbalanced fiber interferometer independantly and actively stabilized [8] by a frequency stabilized laser at a wavelength of 1552 nm (Dicos OFS-2123). Only then is Alice's qubit created. Note that at this point, Bob's photon is already 177 m away from the laboratory.

Once Alice's photon has been encoded, Charlie performs a Bell-State measurement (BSM) jointly with his photon and the photon Alice prepared.

Alignment and Stabilization

Alice's and Charlie's photons need to arrive at the beamsplitter within their coherence time and be indistinguishable for the Bell state measurement to be successful. Charlie's photon passes through a polarization controller to make both polarizations equal at the beamsplitter. Chromatic dispersion is negligible at the 1310 nm wavelength. Charlie filters both photons down to 5 nm of bandwidth, which corresponds to a coherence time of τ_c=500 fs or a coherence length of L_c=150 μm, approximately three times more than the excitation pulse. The easiest way to control the distance traveled by the photons with this precision is add a variable delay consisting of a retroflector mounted on a micrometer step motor placed right after the variable coupler which can move with a precision of 200 nm.

A Mandel Dip [22] experiment (fig. 3) is performed in order to measure the degree of temporal indistinguishability between the two incoming photons. The registered raw visibilities are $V_{00} = 0.255$ and $V_{11} = 0.266$ for the short and long paths respectively. Corrected visibilities are near to the theoretical maximum net visibility of $\frac{1}{3}$[23]. The width of the Mandel Dip, which corresponds to the coherence length of the photons, is 144 μm as expected for filters of 5 nm. Since the fiber spool at Alice's side is longer by one pulse period, the two photons that experience photon bunching have not been created by the same excitation pulse but from subsequent ones.

Unfortunately, the alignment of the different paths is not inherently stable. Temperature fluctuations in the laboratory will affect the length of the fibers and the repetition rate of the laser. In order to avoid length fluctuations of the fiber spools, they have been placed in a common insulated box so that any fluctuation will apply equally to both. The fluctuation in the length difference

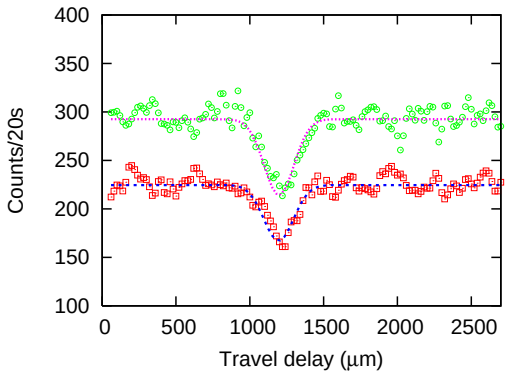


FIG. 3: The circles corresponds to the number of long path coincidences in the coupler, the squares to short path coincidences. Both show a Mandel dip (with visibilities $V_{11} = 0.266$ and $V_{00} = 0.255$ respectively), which demonstrates indistinguishability. Both Mandel dips also are at the same location, demonstrating good alignment of the interferometers.

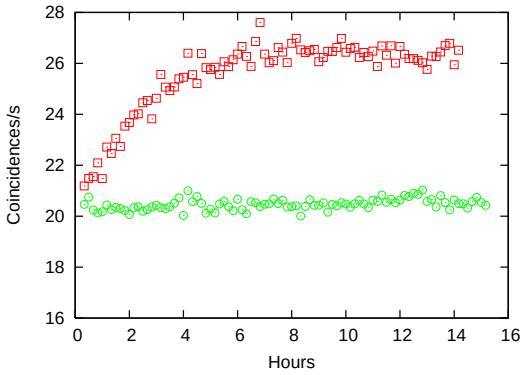


FIG. 4: In squares, the number of counts (sum of short and long paths, normalized) without active stabilization. After a few hours, the coincidence rate has risen to a level equal to that outside the Mandel dip. This means that the photons path lengths are different by more than their coherence length and no bunching occurs. In circles, a similar experiment with active stabilization shows that the indistinguishability condition is now stable. landryfig4.eps

of the nominally equal 177 m spools of fiber has been measured in a Mach-Zender setup to be less than 10 μm. Longer fibers similarly insulated show larger fluctuations: spools of 800 m showed fluctuations of up to 60 μm over less than an hour, which would have destroyed complete indistinguishability on the long term.

There remains two effects that have to be compensated. First, the thermal expansion of the additional 2.72 m of fiber on Charlie's side is not compensated by an equal length on Alice's side as for the other fibers. This 2.72 m will undergo a thermal expansion of $\sim$100 μm/K. Secondly, the laser repetition rate fluctuates in a seemingly random fashion by up to 400 Hz/h in the worst cases, a fluctuation which would cause a change of 15 μm in the additional length needed to skip exactly one period of the laser. These phenomena combined mean that Alice's photon and Charlie's photon will not stay indistinguishable for more than a few hours, not enough to perform a teleportation experiment.

The squares curve in fig. 4 demonstrates this instability. A Mandel dip experiment is performed to find the minimum of the curve as in fig. 3. The motor moves to this point at time zero and is not moved afterwards. It can clearly be seen that the number of coincidences registered increases with time. After a few hours, a plateau is reached where no bunching occurs anymore.

Numerous experiments have shown that the departure from the minimum of the Mandel dip is very well correlated with the repetition rate of the laser which is registered using an external counter (Agilent 53131A). This is because the only parameter involved is the temperature of the laboratory; the laser can then be used as a very sensitive thermometer. It is therefore possible to link the stepmotor movement with the measured repetition rate using a LabView program such that the motor moves at an empirically derived rate of 0.07 μm/Hz. In this way, the step motor position is constantly adjusted for optimal indistinguishability. The results are also shown in fig. 4 in circles.

Another way of stabilizing the length difference would have been to measure the number of coincidences when inside the Mandel Dip and move the motor accordingly in a PID feedback loop. However, due to the low count rate the integration time would have been longer than the observed fluctuation time, making such a system inefficient.

Bell-State Analyzer and electronics

Both 1310 nm photons are sent to a Bell State Analyzer (BSA) consisting of a beam splitter and two detectors (Charlie). One detector is a passive Ge Avalanche Photodiode (APD), the other is a InGaAs APD (IdQuantique Id 200) triggered by the first one.

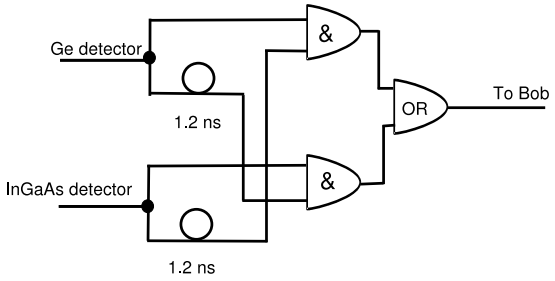


FIG. 5: A schematic of the electronic circuit used to compare the photons time of arrival in the BSA. Each time a photon is detected in each detector with a 1.2 ns delay between each photon, which corresponds to a $|\Psi^-\rangle$ detection, a triggering signal is sent to Bob.

An electronic signal is generated for each photon detection. These signals time arrivals are electronically compared as shown in fig. 5. A $|\Psi^-\rangle$ detection occurs when two photons arrive on different detectors with a time difference of one time-bin, or 1.2 ns in our setup. To reduce dark counts, only those photons which are coincident with a clock signal from the laser are considered. In total, the electronic circuit is able to make a decision whether the signal is a $|\Psi^-\rangle$ in about 220 ns. This time corresponds to the physical cable lengths and various delays that had to be implemented to trigger the active detectors and synchronize and transform the electric signals. When the conditions for a $|\Psi^-\rangle$ are not fulfilled, no information about the state is available. When a $|\Psi^-\rangle$ has been successfully detected, the information is sent to Bob over a second optical fiber (the classical channel) and by means of an optical pulse.

Bob's photon

Bob is at a Swisscom substation at a flight distance of 550 m from the laboratory, but an optical fiber distance of 800 m. Losses in the these fibers are smaller than 2 dB. To minimize chromatic dispersion and reduce spurious detections, the photon is filtered down to a 15 nm width.

Upon receiving the qubit, Bob stores it in a very basic quantum memory consisting of a fiber spool of 250 m waiting for the BSA's information to arrive. Once the confirmation of a successful $|\Psi^-\rangle$ measurement reaches Bob, he opens his InGaAs APD (IdQuantique Id 200) and detects the incoming photon after sending it through an analyzing interferometer. Photons which do not correspond to a successful $|\Psi^-\rangle$ measurement from Charlie are discarded. Arrival times of the photons with respect to the classical signal are measured by means of a Time to Digital Converter (TDC). Timing jitter between the classical information and the qubit is negligible and much smaller than the timing resolution of the InGaAs detector.

By scanning the analyzing interferometer, Bob measures the visibility of the interference in order to extract the fidelity of the teleported state. Bob actively stabilizes his interferometer with a frequency stabilized laser at a wavelength of 1533 nm (Dicos OFS-320).

It is important to note that Bob is a completely independant unit, with its own local interferometer stabilization and controls. A LabView program developped inhouse allows an operator to control Bob, Charlie and Alice from the laboratory using a dedicated TCP/IP channel that uses the third fiber indicated in fig. 2. In particular, the detectors have to be closed when the interferometers are being stabilized; synchronization of the stabilization and measurement periods are made through this channel. Crosstalk between this fiber and the quantum channels is negligible, even at the single-photon level.

Difference between three-photon and four-photon setup

The laser light does not need to be separated equally between the two NLCs and the ratio can be adjusted to minimize noise[8]. When the 1555 nm photon from Alice's NLC is not detected, double pair creation in the EPR source can create a false signal even if there is no photon created in Alice's NLC since it is possible that one photon from the double pair will find its way to the Ge APD and the other one to the InGaAs APD. On the other hand, double pair production in Alice's NLC will not be recorded if there is no corresponding photon at Bob's. Therefore in this case it is usual to use less power on the EPR source than on Alice's source to minimize the number of false counts. However, when the 4^{th} photon is also detected, no false signal will be recorded unless there is also a pair created at Alice's source, therefore we can use equal power on both sources. The resulting noise reduction allows a greater signal-to-noise ratio.

RESULTS

Teleportation without heralded single-photon

A first experiment was performed without detecting the 4^{th} photon to allow a greater count rate. We first performed a Mandel dip to adjust the variable delay and linked its position to the repetition rate of the laser as described before. We locked the phases of the bulk and Alice's interferometer and slowly scanned Bob's interferometer phase. Each point was measured for 53 min to accumulate statistics. The results are shown in fig. 6.

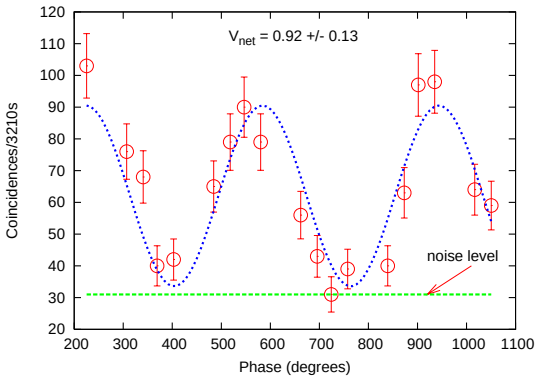


FIG. 6: A teleportation experiment: as we scan the phase of Bob's interferometer, the number of coincidences oscillates, which shows that the qubit is in the expected superposition state. When substracting noise, the near-perfect visibility $V_{net} = 0.92 \pm 0.13$ shows that decoherence is minimal. The raw visibility of $V_{raw} = 0.46 \pm 0.06$ is still higher than the classical limit.

The power on the entangled photon source was low-

ered compared to the power on Alice to reduce noise. The probability of creating a pair of photon per pulse on Alice's NLC was $P_A = 0.19$ and the probability of creating a pair of entangled photon per pulse was $P_B = 0.07$.

The presence of two complete periods shows that the expected cosine is well reproduced. The visibility of the curve and the fidelity[15] $F = (1+V)/2$ are good measures of the quality of the teleportation. The raw visibility $V_{raw} = 0.46 \pm 0.06 (F_{raw} = 0.73 \pm 0.03)$ is higher than the classical limit $V = \frac{1}{3} (F = \frac{2}{3})$. The difference with a perfect visibility comes mainly from known sources of noise such as double pair production in the NLC and dark counts in the detectors. This noise can be measured by running the same experiment but blocking different parts of the signal. When these sources of noise are measured and substracted, we get a net visibility of $V_{net} = 0.92 \pm 0.13$ ($F_{net} = 0.96 \pm 0.06$). We can conclude that decoherence is minimal.

Teleportation with heralded single-photon

Even though the sources of the reduced visibility are known and understood, for practical applications a high raw visibility is needed. We performed a second experiment where we detected the 4^{th} photon to transform Alice into a heralded single-photon source. In this case, the probability of creating a pair was set to be roughly equal in both NLCs at $P = 0.13$. The efficiency of the detector and additional losses induced by the additional optical components meant that the overall signal was reduced by a factor 15, and each point necessitated 6 hrs of data accumulation. However the noise reduction meant that the raw visibility was much higher at $V_{raw} = 0.87 \pm 0.07 (F_{raw} = 0.93 \pm 0.04)$, which is higher than the cloning limit $V = \frac{2}{3} (F = \frac{5}{6})$[24, 25]. The results are shown in fig. 7.

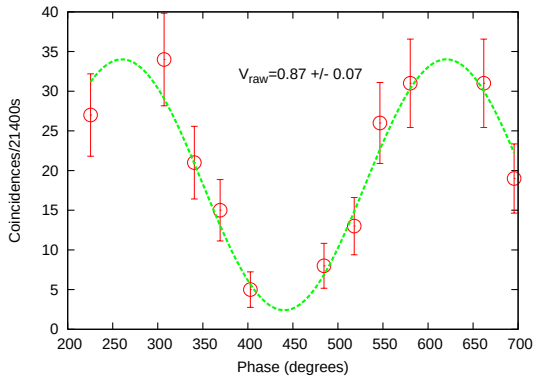


FIG. 7: When taking into account the 4^{th} photon, noise is greatly reduced and we are able to see a raw visibility of $V_{raw} = 0.87 \pm 0.07$.

In this case, the noise is so low as to be unmeasurable by conventional means. Therefore, we did not measure the net visibility. We should point out that in this case, the raw visibility is as high (within uncertainties) as the net visibility of the previous experiment. We can conclude that the main sources of noises can be eliminated by using a heralded single-photon source.

CONCLUSION

In summary, we have performed a teleportation in conditions that are close to field conditions. Bob was a completely independant setup and was remotely controlled. Alice's qubit was created only after the entanglement distribution took place. The necessary optical delays were stabilized using the variations of the repetition rate of the laser, an easily obtainable information. The qubits were created using different pulses of this laser. In the future, using truly independant lasers will enable the construction of a teleportation machine which will have the ability to receive and transport information from another independant machine, an ability which would be helpful in quantum networks for example. Using a heralded single-photon source we were able to obtain a raw fidelity of $F = 0.93 \pm 0.04$.

Acknowledgments

The authors thank Jean-Daniel Gauthier and Claudio Barreiro for their support with the electronic components of this project. This work has been supported by the European Commission under the IST Integrated Project "Qubit Applications" (QAP) and by the Swiss NCCR Project "Quantum Photonics". The authors would like to thank Swisscom for generously giving access to their network and facilities.

[1] C. H. Bennett, F. Bessette, G. Brassard, L. Salvail, and J. Smolin, "Experimental quantum cryptography," Journal of cryptology **5**, 3–28 (1992).

[2] N. Gisin, G. Ribordy, W. Tittel, and H. Zbinden, "Quantum cryptography," Rev. Mod. Phys. **74**, 145–51 (2002).

[3] B. C. Jacobs, T. B. Pittman, and J. D. Franson, "Quantum relays and noise suppression using linear optics," Phys. Rev. A **66**, 052307 (2002).

[4] D. Collins, N. Gisin, and H. De Riedmatten, "Quantum relays for long distance quantum cryptography," Journal of Modern Optics **52**, 735–753 (2005).

[5] H.-J. Briegel, W. Dür, J. I. Cirac, and P. Zoller, "Quantum Repeaters: The Role of Imperfect Local Operations in Quantum Communication," Physical Review Letters **81**, 5932–5935 (1998).

[6] D. Bouwmeester, J.-W. Pan, K. Mattle, M. Eibl, H. Weinfurter, and A. Zeilinger, "Experimental quantum teleportation," Nature **390**, 575–579 (1997).

[7] D. Boschi, S. Branca, F. De Martini, L. Hardy and S. Popescu, "Experimental Realization of Teleporting an Unknown Pure Quantum State via Dual Classical and Einstein-Podolsky-Rosen Channels," Physical Review Letters **80**, 1121–1125, 1998

[8] I. Marcikic, H. de Riedmatten, W. Tittel, H. Zbinden, and N. Gisin, "Long-distance teleportation of qubits at telecommunication wavelengths," Nature **421**, 509–513 (2003).

[9] R. Ursin, T. Jennewein, M. Aspelmeyer, R. Kaltenbek, M. Lindenthal, P. Walther, and A. Zeilinger, "Quantum Teleportation across the Danube," Nature **430**, 849 (2004).

[10] C. Bennett, G. Brassard, C. Crépeau, R. Jozsa, A. Peres, and W. Wootters, "Teleporting an unknown quantum state via dual classical and Einstein-Podolsky-Rosen channels," Phys. Rev. lett. **70**, 1895 (1993).

[11] J. van Houwelingen, N. Brunner, A. Beveratos, H. Zbinden, and N. Gisin, "Quantum Teleportation with a 3-Bell-state Analyzer," PRL **96**, 130,502 (2006).

[12] A. Einstein, B. Podolsky, and N. Rosen, "Can Quantum-Mechanical Description of Physical Reality Be Considered Complete?" Phys. Rev. **47**, 777–780 (1935).

[13] J. Brendel, N. Gisin, W. Tittel, and H. Zbinden, "Pulsed Energy-Time Entangled Twin-Photon Source for Quantum Communication," Phys Rev. Lett. **82**, 2594 (1999).

[14] R. T. Thew, S. Tanzilli, W. Tittel, H. Zbinden, and N. Gisin, "Experimental investigation of the robustness of partially entangled qubits over 11 km," Phys. Rev. A **66**, 062304 (2002).

[15] H. de Riedmatten, I. Marcikic, W. Tittel, H. Zbinden, D. Collins, and N. Gisin, "Long Distance Quantum Teleportation in a Quantum Relay Configuration," Phys. Rev. Lett. **92**, 047904 (2004).

[16] H. de Riedmatten, I. Marcikic, J. A. W. van Houwelingen, W. Tittel, H. Zbinden, and N. Gisin, "Long-distance entanglement swapping with photons from separated sources," Phys. Rev. A **71**, 050302(R) (2005).

[17] W. Tittel and G. Weihs, "Photonic entanglement for fundamental tests and quantum communication," QIC **1**–**56**, 3 (2001).

[18] S. Fasel, O. Alibart, S. Tanzilli, P. Baldi, A. Beveratos, N. Gisin, and H. Zbinden, "High-quality asynchronous heralded singe-photon source at telecom wavelength," New Journ. Phys. **6**, 163 (2004).

[19] T. Pittman, B. Jacobs, and J. Franson, "Heralding Single Photons from Pulsed Parametric Down-Conversion," Opt. Comm. **246**, 545–550 (2004).

[20] T. Yang, Q. Zhang, T.-Y. Chen, S. Lu, J. Yin, and J.-W. Pan, "Experimental Synchronization of Independent Entangled Photon Sources," Physical Review Letters **96**, 110,501 (2006).

[21] R. Kaltenbaek, B. Blauensteiner, M. Zukowski, M. Aspelmeyer, and A. Zeilinger, "Experimental interference of independant photons," (2006). quant-ph/0603048.

[22] C. K. Hong, Z. Y. Ou, and L. Mandel, "Measurement of subpicosecond time intervals between two photons by interference," Phys. Rev. Lett. **59**, 2044–2046 (1987).

[23] H. de Riedmatten, I. Marcikic, W. Tittel, H. Zbinden, and N. Gisin, "Quantum interference with photon pairs created in spatially separated sources," Phy. Rev. A **67**, 022301 (2003).

[24] F. Grosshans and P. Grangier, "Quantum cloning and teleportation criteria for continuous quantum variables," Phys. Rev. A **64**, 010301 (2001).

[25] D. Bruß, D. DiVincenzo, A. Ekert, C. Fuchs, C. Macchiavello, and J. Smolin, "Optimal universal and state-dependent quantum cloning," Phys. Rev. A **57**, 2368–2378 (1998).